Proceedings of 9th IEEE International Conference
on CYBER Technology in Automation, Control, and Intelligent Systems
July 29- August 2, 2019, Suzhou, China

Design, Prototype, and Control Design Based on Computed Torque Control of Selective Compliance Assembly Robot Arm

Ahmad Albalasie[1,*], Irfan Hussain[2], *Member, IEEE*, Mamon Horoub[3], Sikandar Khan[3], Sajid Ali[4], Dongming Gan[2], *Member, IEEE*

***Abstract*— This paper presents the design, the prototype and the control of SCARA (Selective Compliance Assembly Robot Arm) to perform pick and place tasks for industrial applications. The robot has four degrees of freedom (DoFs) with a capability to carry payloads up to 1 kg with high accuracy, precision, and repeatability. The robot is designed using the CAD tools and its prototype development is carried out by manufacturing its mechanical parts (links, base) and selecting the proper off the shelf electrical (motors, controllers) and transmission components (belts, pulleys). We also present the mathematical formulation consisting of direct kinematics, inverse kinematics, and the dynamical equations of the robot. We also report a closed loop position control based on the Computed Torque Control (CTC) method. The Numerical simulations are performed in order to evaluate the performance of the robot by using the applied control technique. The future work includes the experiments on the hardware using the implemented control technique.**

I. INTRODUCTION

Robotics applications are rapidly growing for humans' assistance [1,2] and in industrial applications [3]. In this direction, different types of actuation ranging from passive to active control techniques and fabrications methods are presented in the literature [4, 5]. The huge expand of industrial fields around the world with increasing demand on executing dangerous tasks, repeatable production tasks with demand also on increasing the productivity are forcing the industry of robots to get a higher level to achieve the required goals.

For this reason, the robots are becoming one of the basic and major components of the most developed factories. The growing demands of huge production rate in factories are certainly not possible by human workers only. To meet this challenge, the robots are participating in this mission day by day. At one end, integrating more industrial robots in the production lines are increasing the productivity of these lines with improved product quality, accuracy and precision. On the other hand, it is decreasing the production cost. The SCARA robot is one of the most widely used robot in industry to be used for pick and place applications. Design and development of this robot at small scale can provide an amazing learning opportunity in educational institutions and labs. Nevertheless, since these robots are normally very expensive industrial products and out of the budgets of universities and students. Moreover, it is difficult to find the design guidelines and prototyping techniques of such robots due to product confidentiality. Thus, building such robots and providing the design guidelines at small scale can open new learning opportunities for students and educational institutions, which motivated us for this study.

The SCARA provides consistent reliable performance, repetitive accuracy and ability to handle light payloads and to perform different tasks in harsh environments. Needless to mention, it can be reprogrammed to reflect changes in production lines. It guarantees high performance in term of productivity and at the same time high flexibility in assembly lines and production lines. This robot is used in a wide variety of processes and applications, such as production equipment for electrical and electronic components, and small precision "machine components requiring the precise assembly, and assembly, handling, and transfer of large automotive components. The SCARA has four DoFs in which two or three horizontal servo-controlled joints are shoulder, elbow, and wrist. An actuator controls last vertical axis with power screw mechanism. The tasks performed can be classified as pick and place, non-contact tasks (welding, painting) and the contact tasks (peg-in-hole).

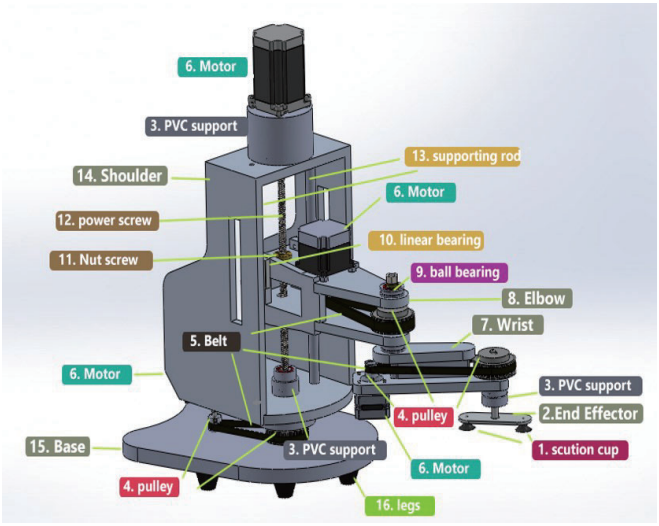

Figure 1: The CAD representation and a major component of the designed SCARA robot.

SCARA designed at Japan, is generally suited for small parts insertion tasks for assembly lines like electronic component insertion [6–8]. Many different studies have been carried out on SCARA robot. Bhatia et al. have implemented an expert system-based approach for the design of a SCARA robot [9]. Ge et al. have presented dynamic modelling and controller design for a SCARA/Cartesian smart materials

[1,*]Contacting Author: Ahmad Albalasie is with Department of Mechanical and Mechatronics Engineering, Birzeit University, Birzeit, PO Box 14, Palestine (Tele: +970-2-298-2000 -Ext:2115, Fax: +970-2-281-0656; E-mail: abalasie@birzeit.edu).

[2]Irfan Hussain and Dongming Gan are with Khalifa University Center for Autonomous Robotic Systems (KUCARS), Khalifa University of Science and Technology, Abu Dhabi, United Arab Emirates.

[3]Department of Mechanical Engineering, King Fahd University of Petroleum and Minerals, Dhahran, 31261, Saudi Arabia.

[4]Mechanical and Energy Engineering Department, Imam Abdulrahman bin Faisal University, Dammam 31441, Saudi Arabia.

978-1-7281-0770-7/19/$31.00 ©

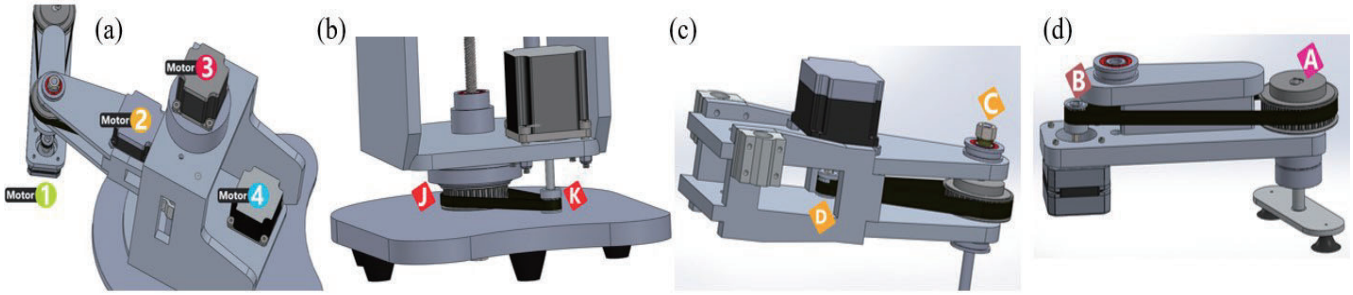

Figure 2: The CAD views of different parts of the robot. The motors locations on the robot structure (a). Mechanisms of different joints i.e. Base (b), wrist (c) and end effector (d). Each consists of a motor, two pulleys and a belt.

robot with piezoelectric actuators and sensors [10]. Omodei et al. have presented and compared three algorithms for the geometric parameter identification of industrial robots [11]. Experimental results were obtained for a SCARA IBM 7535 robot. A CRS A 251 robot was simulated with TELEGRIP software. Er et al. have then studied on the design, development and implementation of a Hybrid Adaptive Fuzzy Controller (HAFC) suitable for real-time industrial applications [12]. The SEIKO D-TRAN 3000 series SCARA robot was controlled and analyzed. Hong et al. have investigated a modular and object oriented [13].

In this paper, we present the design, the prototype and the control of SCARA robot to perform pick and place tasks for industrial applications. The robot has four degrees of freedom (DoFs) with a capability to carry payloads up to 1 kg. A closed loop position control is implemented using computed torque control technique. In order to evaluate the performance of the applied control technique on the robot, we performed the numerical simulation.

The rest of the paper is organized as it follows: The design and the development are detailed in section 2. Section 3 reports the forward kinematics, the inverse kinematics, and the dynamics of the robot. Section 4 presents the closed loop trajectory control scheme based on the CTC. Next, section 5 presents the numerical example to evaluate the control scheme. Finally, conclusion and future work are outlined in section 6.

II. Design and Development

The CAD representation of the complete assembled robot and its major components is shown in Figure 1. While, Figure 2 reports the mechanisms of different joints. The robot has four DOFs: the first joint on the base is a revolute joint [R] while the second joint is prismatic joint [P] and the other two joints are revolute joints [RR]. In the remaining part of this section, we present the calculations performed for the proper selection of the parts of the robot i.e. motor torque, pulleys selection procedure, belt length etc. Moreover, we present the electronic components of our system along with their interfaces.

A. The Required Torque for the Motors

The end effector (EE) actuation consists of a motor, pulleys and timing belt. To find the torque that the motor should apply to rotate the EE, desired values for the speed of EE and time needed to reach maximum speed are chosen to be 30 rpm (3.14 rad/sec) and 0.5 second respectively. Using these values, the angular acceleration ($\propto_A$) is calculated 6.28 rad/s^2.

In order to find the required torque that motor must apply, gear ratio must be considered since power is transferred by a timing belt from the motor shaft to the EE shaft using two pulleys as shown in Figure 2.d. The selected pulleys have the following number of teeth.

Number of teeth of Pulley A (N_A) = 32

Number of teeth of Pulley B (N_B) = 10

So, the speed of pulley B (n_B) is 96 rpm, which is calculated by (1):

$$n_B = n_A \frac{N_A}{N_B} \quad (1)$$

The required torque at pulley 'A' is determined as follows:

$$T_A = I_A \times \propto_A \quad (2)$$

Where:

I_A: the total mass moment of inertia for the EE with the maximum load at point A. It is recommended to clarify I_A is computed using SolidWorks so $I_A = 2.7 * 10^{-3}\ kg.m^2$.

T_A: is the torque at the pully A side.

$\propto_A$: is the angular acceleration at pully A side.

Based on that, the torque at pulley A (T_A) is 1.7*10^{-2} N.m. which is computed using (2). Now to calculate the motor torque (T_B), it is necessary to take into account the gear ratio and the efficiency of the timing belt as shown in (3).

$$T_B = \frac{T_A}{\eta \frac{N_A}{N_B}} \quad (3)$$

Where:

η: is the timing belt efficiency which is equal to 0.91.

Consequently, the required torque for the motor (T_B) is given by 6*10^{-3} N.m.

Finally, the same procedures are repeated for each actuator to compute the required torque. Thus, Table I reports the capabilities of the selected motors based on the maximum speed and the maximum torque after taking into account the factor of safety which is selected as 2.

B. Pulleys Selection Process

The selection process for the tooth profile for pulleys and belts depend on the design power transmitted by belt from one pulley to the other one and on the speed of belt. Using the values of power and speed, the tooth profile can be selected using design charts. To find the transmitted power in the belt (4) is used:

$$Pt = T \times \omega \quad (4)$$

Where:
Pt: transmission power.
T: input torque.
ω: input speed.

TABLE I. THE CHARACTERISTS OF THE SELECTED MOTORS

Motor No.	Max. Torque	Max. Speed
1	0.012	192
2	0.2	94
3	1.8	1125
4	0.34	192

Selecting the tooth profile requires to use the design power not the transmission power. So, a factor of safety is used to convert the transmission into design power as shown in (5). This factor of safety is called a service factor that depends on three other factors as illustrated in (5) and (6).

$$Pd = Pt \times K_s \quad (5)$$

Where:
Ks: Service factor.
Pd= Design power.

$$K_s = K_o + K_r + K_i \quad (6)$$

Where:
K_o: Service correction factor.
K_r:Speed ratio correction factor.
K_i:Idler correction factor.
Table II show the technical specifications for the selected pulleys A and B.

TABLE II. TECHNICAL SPECIFICATIONS OF PULLEYS A & B

Item	Technical Specifications	
	Pully A	***Pully B***
Tooth Style	XL	XL
Belt Width [mm]	0.375	0.375
Material	AL	AL
Bore [mm]	12	6
P.D [mm]	51.7	16.2
O.D [mm]	51.2	15.7

C. *Belt Length*

The total length of the EE belt between pulleys A and B is 424.34 mm and it is computed by (7).

$$L_p = 2C + \frac{\pi(D_p + d_p)}{2} + \frac{\pi(D_p - d_p)^2}{4C} \quad (7)$$

Where:
L_p: belt length (mm).
C: center distance (mm).
D_p: large pulley pitch diameter (mm).
d_p: small pulley pitch diameter (mm).

Now the same procedures are repeated to design the pulleys, the timing belts, and for the selection of suitable motors for the wrist and the base. While there are small modifications for the shoulder because a power screw mechanism is used. The complete assembled prototype of the robot is shown in Figure 3.

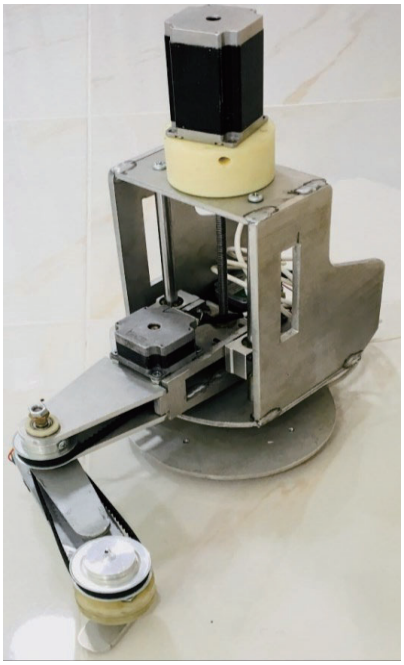

Figure 3. The Complete Assembled Prototype of the Robot.

D. *Electronics Hardware and Controller*

In this project, a PC is used to control the robot. Therefore, an Arduino Mega kit is used as data acquisition system to convertor the digital signals into the analog signals and the vice versa. This kit is selected because it is cost effective and it has the capability to communicate with PC using FTDI cable. In addition; a closed loop control scheme is designed based on CTC is used to control the system. This scheme was built in LABVIEW software to control the system on PC. Consequently, two types of motor drivers are selected for driving the selected motors as shown in Figure 4.

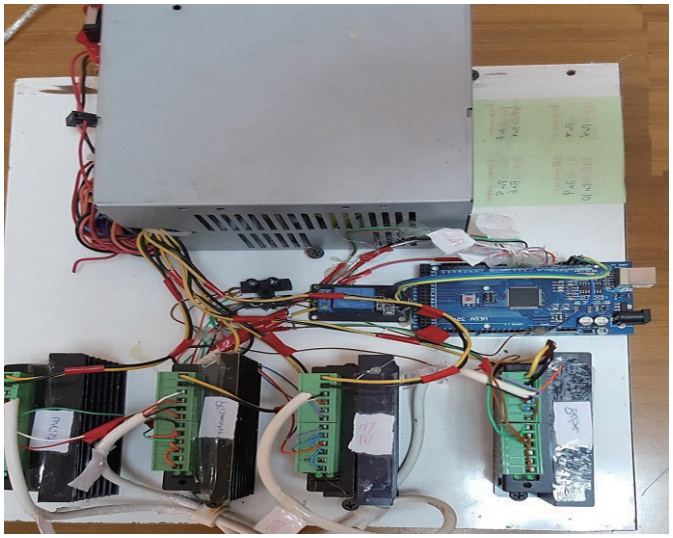

Figure 4: Electrical and electronics circuits

III. KINEMATICS AND DYNAMICS

This section presents the direct, inverse kinematics and the dynamics of the proposed system.

A. Direct Kinematics

The kinematics of the robot is described by its DH parameters. Considering, the geometric configuration of our robot as shown in Figure 5, the corresponding DH parameters are listed in Table III.

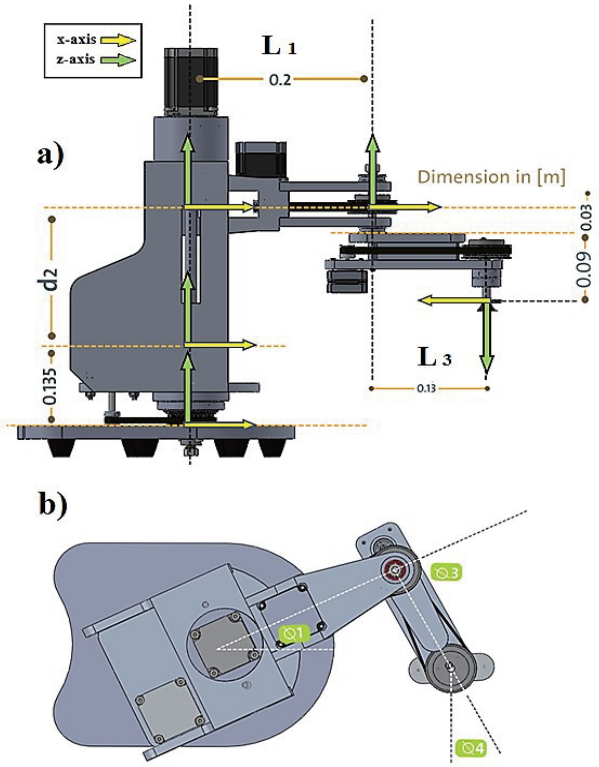

Figure 5: Geometric configuration a) Isometric view b) Top view

TABLE III. DH- PARAMETERS FOR SCARA

i	α_{i-1}	a_{i-1}	θ_i	d_i
1	0	0	θ_1	0.0135
2	0	0	0	d_2
3	0	0.20	θ_3	0
4	-π	0.13	θ_4	-0.12

Based on that, each T_i^{i-1} is computed and the overall transformation matrix (T_4^0) is shown in (8).

$$T_4^0 = \begin{bmatrix} cq_{134} & sq_{134} & 0 & 0.20cq_{13} + 0.13cq_{134} \\ sq_{134} & -cq_{134} & 0 & 0.20sq_{13} + 0.13sq_{134} \\ 0 & 0 & -1 & q_2 + .015 \\ 0 & 0 & 0 & 1 \end{bmatrix} \quad (8)$$

B. Inverse Position Kinematics

The pose of the end-effector is given by (9-12)

$$X_e = l_1 cq_1 + l_3 cq_{13} \quad (9)$$

$$Y_e = l_1 sq_1 + l_3 sq_{13} \quad (10)$$

$$Z_e = q_2 + d_0 \quad (11)$$

$$\emptyset_e = q_1 + q_3 + q_4 \quad (12)$$

To find the joint variables (13) is used.

$$X_e^2 + Y_e^2 = \Delta_1 \quad (13)$$

Where: $\Delta_1 = l_1^2 + l_3^2 + 2l_1 l_3 cq_3$

Thus,

$$cq_3 = \left(\frac{X_e^2 + Y_e^2 - l_1^2 - l_3^2}{2l_1 l_3}\right) \quad (14)$$

Eq's (9-10) can be written as follow:

$$X_e = cq_1\Delta_2 - sq_1(l_3 sq_3) \quad (15)$$

$$Y_e = sq_1\Delta_2 + cq_1(l_3 sq_3) \quad (16)$$

Where $\Delta_2 = (l_1 + l_3 cq_3)$.

Eq. (16) also can be written as shown in (17):

$$sq_1 = \frac{Y_e - cq_1(l_3 sq_3)}{\Delta_2} \quad (17)$$

By substituting (17) into (15) the result is shown in (18)

$$cq_1\Delta_2 = X_e + \left(\frac{Y_e - cq_1(l_3 sq_3)}{\Delta_2}\right)(l_3 sq_3) \quad (18)$$

This is yields also to (19)

$$cq_1\Delta_2^2 = X_e\Delta_2 + \left(Y_e - cq_1(l_3 sq_3)\right)(l_3 sq_3) \quad (19)$$

By rearrange the (19) this is yields to:

$$cq_1 = \frac{X_e\Delta_2 + Y_e(l_3 sq_3)}{\Delta_1} \quad (20)$$

Substitute (20) into (17)

$$sq_1\Delta_2 = Y_e - \left(\frac{X_e\Delta_2 + Y_e(l_3 sq_3)}{\Delta_1}\right)(l_3 sq_3) \quad (21)$$

$$sq_1\Delta_2\Delta_1 = Y_e\Delta_1 - \left(X_e\Delta_2 + Y_e(l_3 sq_3)\right)(l_3 sq_3) \quad (22)$$

After simplifying (22) the result is shown in (23):

$$sq_1 = \frac{Y_e\Delta_2 - X_e(l_3 sq_3)}{\Delta_1} \quad (23)$$

$$q_1 = atan2(sq_1, cq_1) \quad (24)$$

$$q_2 = Z_e + d_0 \quad (25)$$

$$q_4 = \emptyset_e - q_1 - q_3 \quad (26)$$

C. Dynamics

The dynamics of robot is the relationships between the torques applied to the joints and the consequent movements of the links. The dynamics equations for the robot is derived by using the Lagrange algorithm where the mass moment of inertia for each link is estimated by SolidWorks software. The resultant dynamic equations of the robot are detailed in the following:

$$\begin{aligned} \tau_1 = {} & 3.615\,\ddot{q}_1 + 0.109\,\ddot{q}_3 - 0.0516\,\ddot{q}_4 \\ & - 0.0055\,\dot{q}_3^2\,s(q_3) + 0.061\,\ddot{q}_1 c(q_3) \\ & + 0.03\,\ddot{q}_3\,c(q_{34}) + 0.03\,\ddot{q}_4\,c(q_{34}) \\ & + 0.011\,\ddot{q}_1 cos(q_3) + 0.005\,\ddot{q}_3\,c(q_3) \\ & - 0.03\,\dot{q}_3^2\,s(q_{34}) - 0.03\,\dot{q}_4^2\,s(q_{34}) \\ & - 0.011\,\dot{q}_1\dot{q}_3\,s(q_3) - 0.06\,\dot{q}_1\dot{q}_3\,s(q_{34}) \\ & - 0.06\,\dot{q}_1\dot{q}_4\,s(q_{34}) - 0.06\,\dot{q}_1\dot{q}_4 s(\theta_{34}) \end{aligned} \quad (27)$$

$$\tau_2 = 2.741\,\ddot{q}_2 - 26.889 \quad (28)$$

$$\tau_3 = 0.109\,\ddot{q}_1 + 0.109\,\ddot{q}_3 \quad (29)$$

$$
\begin{gathered}
-0.0516\ \ddot{q}_4 + 0.0055\ \dot{q}_1^2\ s(q_3) \\
+\ 0.030\ \ddot{q}_1\ c(q_{34}) + 0.0055\ \ddot{q}_1 c(q_3) \\
+\ 0.03\ \dot{q}_1^2\ s(q_{34})
\end{gathered}
$$

$$
\begin{gathered}
\tau_4 = 0.03\ \dot{q}_1^2\ s(q_{34}) - 0.052\ \ddot{q}_1 - 0.0\ \ddot{q}_3 \\
+ 0.097\ \ddot{q}_4 + 0.03\ \ddot{q}_1 \ddot{\theta}_1 c(q_{34})
\end{gathered} \tag{30}
$$

IV. Control

The control technique implemented is the computed torque control (CTC) which is classified as model-based control. Thus, we design a trajectory-following controller that tracks the desired position, the desired velocity, and the desired acceleration which provide a closed loop control with the desired frequency ω_{ni_des} and a desired damping ration ζ_{i_des} for each joint separately. This is achieved by understanding the general form for the dynamics equations as shown in (31):

$$M(q) + V(q, \dot{q}) + G(q) = T \tag{31}$$

To make the system as unity mass and linear system as shown in (32-34):

$$T = \alpha \grave{T} + \beta \tag{32}$$

$$\alpha = \hat{M}(q) \tag{33}$$

$$\beta = \hat{V}(q, \dot{q}) + \hat{G}(q) \tag{34}$$

Where:
α is the term that converts the system to unit mass system.
β is term that makes the system a linear system
$\hat{M}$: is the estimated mass matrix.
$\hat{G}$: is the estimated gravity vector.
$\hat{V}$: is the estimated Coriolis and Centrifugal vector.

By Substituting (32-34) into (31) with a perfect estimation process. This yields to the following dynamic equations:

$$\ddot{\boldsymbol{q}} = \grave{\boldsymbol{T}} \tag{35}$$

Where $\grave{\boldsymbol{T}}$ is given by:

$$\grave{\boldsymbol{T}} = \ddot{\boldsymbol{q}}_{\boldsymbol{d}} - \overline{\boldsymbol{k}}_{\boldsymbol{v}}(\dot{\boldsymbol{q}} - \dot{\boldsymbol{q}}_{\boldsymbol{d}}) - \overline{\boldsymbol{k}}_{\boldsymbol{p}}(\boldsymbol{q} - \boldsymbol{q}_{\boldsymbol{d}}) \tag{36}$$

This yields for the following equations:

$$\ddot{\boldsymbol{e}} + \overline{\boldsymbol{k}}_{\boldsymbol{v}}\dot{\boldsymbol{e}} + \overline{\boldsymbol{k}}_{\boldsymbol{p}}\boldsymbol{e} = \boldsymbol{0} \tag{37}$$

Where:
$\overline{\boldsymbol{k}}_{\boldsymbol{p}}$: is a diagonal proportional gain matrix.
$\overline{\boldsymbol{k}}_{\boldsymbol{v}}$: is a diagonal derivative gain matrix.

V. Numerical Simulation

In this section, we present the numerical simulation based on the dynamic model and control technique detailed in previous sections. A cubic trajectory planning algorithm in the joint space is used to create a trajectory for each joint to move from one point to another point. Consequently, Figures (6-9) show a comparison between the desired response and the simulated response for each joint of the robot. As it can be seen in the Figures, the applied control technique showed its capability to track the desired responses without any significant error except a small error in the third joint. Furthermore, the time required to perform the motion was only two seconds as shown in the Figures.

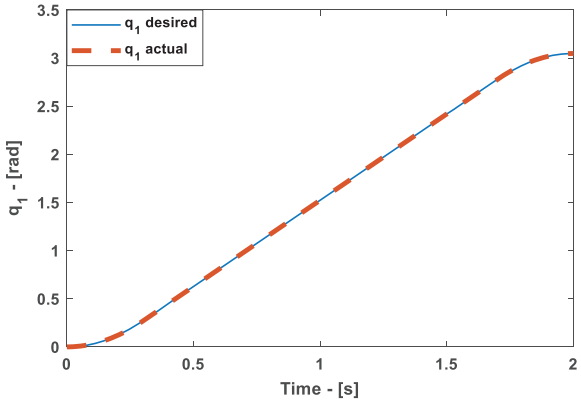

Figure 6: A comparison between the desired response and the simulated response for the first joint

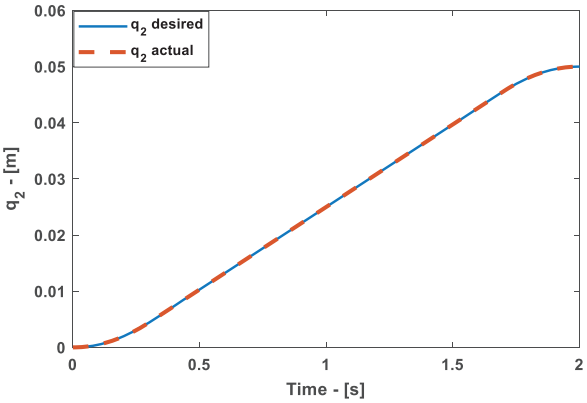

Figure 7: A comparison between the desired response and the simulated response for the second joint

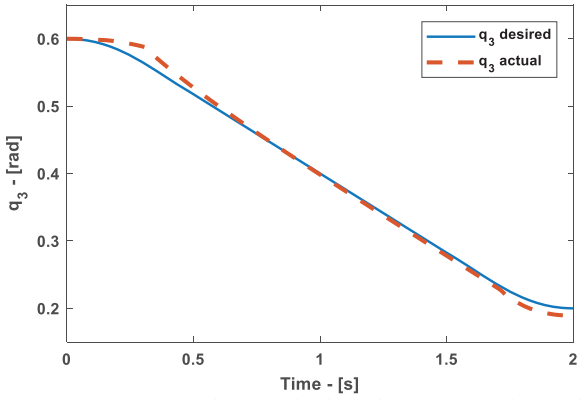

Figure 8: A comparison between the desired response and the simulated response for the third joint

VI. Conclusions

This paper presented the design guidelines, prototype, kinematics, dynamic model and control of an educational prototype of a SCARA. A careful selection of the electrical parts (e.g. motors, drivers, controllers) and mechanical transmission parts (belts, pulleys) is carried out after performing calculations. The detailed forward kinematics,

inverse kinematics and the dynamics of the robot are presented to be used in the control stage and better understand its behavior. We performed numerical simulations based on the Computed Torque Control technique in order to evaluate the performance of the robot model and implemented control technique. In future, we are aiming to perform further experiments on the prototype of the developed robot. We believe the development of such low-cost platforms can provide excellent learning opportunities in the educational institutions.

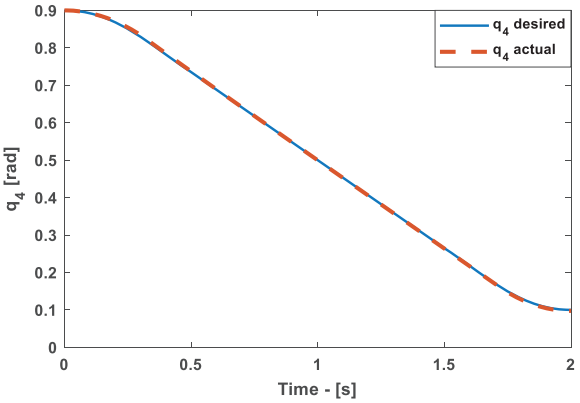

Figure 9: A comparison between the desired response and the simulated response for the fourth joint

REFERENCES

[1] I. Hussain, G. Salvietti, G. Spagnoletti, and D. Prattichizzo, "Thesoft-sixthfinger: a wearable emg controlled robotic extra-finger forgrasp compensation in chronic stroke patients,"IEEE Robotics andAutomation Letters, vol. 1, pp. 1000 –1006, July 2016

[2] I. Hussain, G. Spagnoletti, G. Salvietti, and D. Prattichizzo, "Towardwearable supernumerary robotic fingers to compensate missing grasp-ing abilities in hemiparetic upper limb,"The International Journal ofRobotics Research, vol. 36, no. 13-14, pp. 1414–1436, 2017.

[3] Engelberger, Joseph F. Robotics in practice: management and applications of industrial robots. Springer Science & Business Media, 2012.

[4] I. Hussain, A. Albalasie, M. I. Awad, L. Seneviratne, and D. Gan, "Modeling, control and numerical simulations of a novel binarycontrolled variable stiffness actuator (bcvsa)," Frontiers in Robotics and AI, vol. 5, p. 68, 2018.

[5] I. Hussain, F. Renda, Z. Iqbal, M. Malvezzi, G. Salvietti, L. Seneviratne, D. Gan, and D. Prattichizzo, "Modeling and prototyping of an underactuated gripper exploiting joint compliance and modularity," IEEE Robotics and Automation Letters, vol. 3, pp. 2854–2861, Oct 2018.

[6] R.C. Dorf, Concise International Encyclopedia of Robotics—Applications and Automation, John Wiley and Sons Inc., 1990.

[7] S.Y. Nof, Handbook of Industrial Robotics, John Wiley and Sons, 1985.

[8] R.I. Eugene, Mechanical Design of Robots, McGraw-Hill, 1988.

[9] P. Bhatia, J. Thiunarayanan, N. Dave, An expert system-based design of SCARA robot, Expert Systems with Applications 15 (1998) 99–109.

[10] S.S. Ge, T.H. Lee, J.Q. Gong, A robust distributed controller of a single-link SCARA/Cartezian smart materials robot, Mechatronics 9 (1999) 65–93.

[11] A. Omodei, G. Legnani, R. Adamini, Three methodologies for the calibration of industrial manipulators: experimental results on a SCARA robot, Journal of Robotic Systems 17 (6) (2000) 291–307.

[12] M.J. Er, M.T. Lim, H.S. Lim, Real time hybrid adaptive fuzzy control of a SCARA robot, Microprocessors and Microsystems 25 (2001) 369–378.

[13] K.S. Hong, K.H. Choi, J.G. Kim, S. Lee, A PC-based open robot control system: PC-ORC, Robotics and Computer Integrated Manufacturing 17 (2001) 355–365.

[14] "Pfeifer Industries, Timing belt advantages and disadvantages" http://www.pfeiferindustries.com/timing-belt-advantages-disadvantages-i-15-l-en.html. Accessed: 2019-01-23.

[15] "Mat Web: Material Property Data" http://www.matweb.com/search/DataSheet.aspx?MatGUID=626ec8cdca604f1994be4fc2bc6f7f63&ckck=1. Accessed: 2019-01-23.